International Conference on Applied Energy 2020
Dec. 1 - Dec. 10, 2020, Bangkok / Virtual
Paper ID: 0146

Numerical simulation of closed-loop heat extraction from deviated-geothermal wells

Yuncheng Gu[1,2], Xinli Lu[1,2]*, Jiaqi Zhang[1,2], Jiali Liu[1,2], Zhiwei Cui[1,2], Hao Yu[1,2], Changyou Geng[1,2], Yapeng Ren[1,2]

[1] Tianjin Geothermal Research and Training Center, Tianjin University, Tianjin 300350, P.R.China

[2] Key Laboratory of Efficient Utilization of Low and Medium Grade energy, MOE, Tianjin University, Tianjin 300350, P.R. China

* Corresponding author. Tel.: +86-18522972804, Email address: xinli.lu@tju.edu.cn

ABSTRACT

As closed-loop heat extraction technology can be used for both "dry" and "wet" geothermal wells, it is getting more and more attention from engineers and scientists. In this study, numerical simulation has been carried out to investigate the performances of closed-loop heat extraction models for a vertical geothermal well (Model A), a deviated geothermal well (Model B), and symmetrically arranged two deviated-geothermal wells (Model C). Comparisons of the performances have been made among the three models. The changes of outflow temperature and heat extraction rate with respect to different mass flow rates were analyzed in detail. Results show that the Model C has an obvious advantage over the Model A and Model B. The heat extraction rate of Model C is 155 kW at the flowrate of 3kg/s at the end of 4 months, which has increased by 124% compared to the Model A and 94% compared to the Model B. Results obtained is considered to be useful for a better understanding of closed-loop heat extraction systems.

Keywords: closed-loop heat extraction, deviated-geothermal wells, numerical simulation

1. INTRODUCTION

Exploiting the renewable energy rather than fossil fuels has become increasingly important. Among all types of renewable energy, geothermal energy is an ideal choice [1]. It can be used for heating and generating electricity and has advantages over wind and solar power [2, 3]. Closed-loop technology can be used to effectively extract heat from the underground formation and can avoid problems of corrosion, scaling in the wellbore, and mass flowrate loss in the reservoir [4]. Rybach and Hopkirk, firstly proposed the concept of using coaxial heat exchanger to provide heat for buildings in 1995 [5]. Alimonti et al. once set up a numerical model of a coaxial heat exchanger to maximize the extracted heat on Villafortuna Trecate oilfield [6]. Bu et al. made a study on acquiring geothermal energy from an abandoned oil and gas well using coaxial heat exchanger and verified its feasibility [7]. Noorollahi et al. carried out a numerical simulation of two vertical closed-loop heat extraction models for two oil wells in southern Iran [8].

However, few studies investigated the performance of closed-loop heat extraction from deviated-geothermal wells. In this paper, Closed-loop heat extraction models for a vertical geothermal well (Model A), a deviated geothermal well (Model B) and symmetrically arranged two deviated-geothermal wells (Model C) have been established. Their heat extraction performances were compared with respect to different inflow parameters.

2. MODELS

2.1 Three closed loop heat extraction models

The layout and configurations of three closed-loop heat extraction models are shown in Fig.1 (a), (b) and (c). The working fluid flows downward in the annular space, absorbing heat from the formation, and then flows upward through the inner pipe to the outlet. It is important to note that in the Model C, the deviated segment of both outer pipe and inner pipe is equally divided into two symmetrical parts according to mass conservation. Thus, working fluid is divided into two branches evenly before flowing into deviated annular space, and they will join together when flowing up into the vertical segment of the inner pipe. Such scheme will largely expand the heat transfer area between working

Selection and peer-review under responsibility of the scientific committee of the 12th Int. Conf. on Applied Energy (ICAE2020).

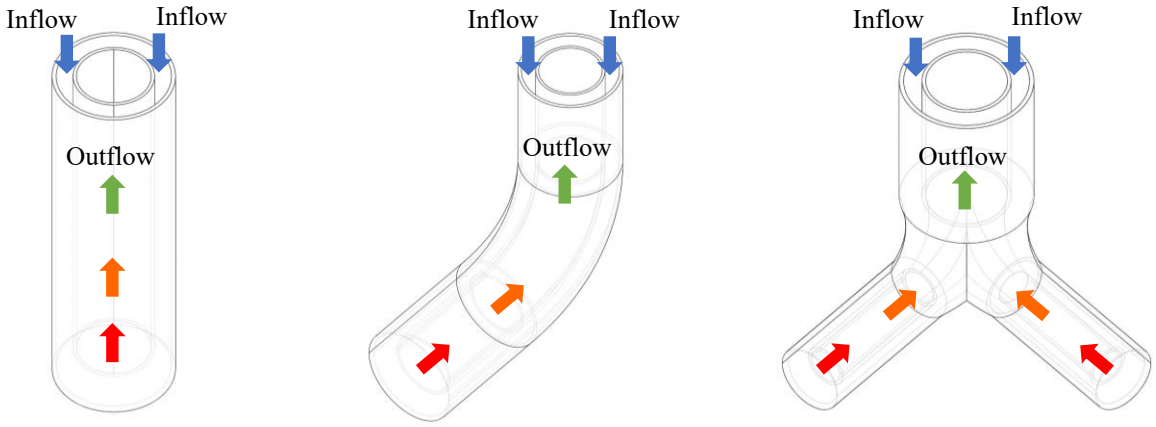

(a) Model A (b) Model B (c) Model C

Fig.1 Closed-loop heat extraction models for a vertical geothermal well (a), a deviated geothermal well (b), and symmetrically arranged two deviated-geothermal wells (c)

fluid and the formation. In order to do the simulation under a 2D condition, a simplified Model C was established. as shown in Fig.2. Here, the vertical segment was also equally divided into two symmetrical parts according to the mass conservation.

The simulation was carried out by using Fluent. In each of the three models, the inner pipe wall is assumed to be well insulated and the outer pipe wall is coupled with the corresponding formation in terms of heat balance. Water is used as working fluid and the formation is divided into four layers. The geothermal gradient used in the simulation is valued as 30°C/km. The length of vertical segment of the well is set to be 1000m. According to the Geothermal Well Test Analysis [10], the radius of curvature is set to be 400m and the angle of inclination is set to be 40°, as shown in Fig.3. Such a closed loop actually forms a coaxial heat exchanger which can expand the heat transfer area. In the following part of this paper, each of the models will be considered as a coaxial heat exchanger. The parameters of the coaxial heat exchanger corresponding to each model and the properties of each formation layer are shown in Table 1 and Table 2 respectively. The data was partly adopted from the study of Cai et al [9] in order to validate the model.

2.2 Model validation

Here we use the experimental data from Cai [9] to verify the accuracy of the Model A. The comparison between measured and simulated results are shown in

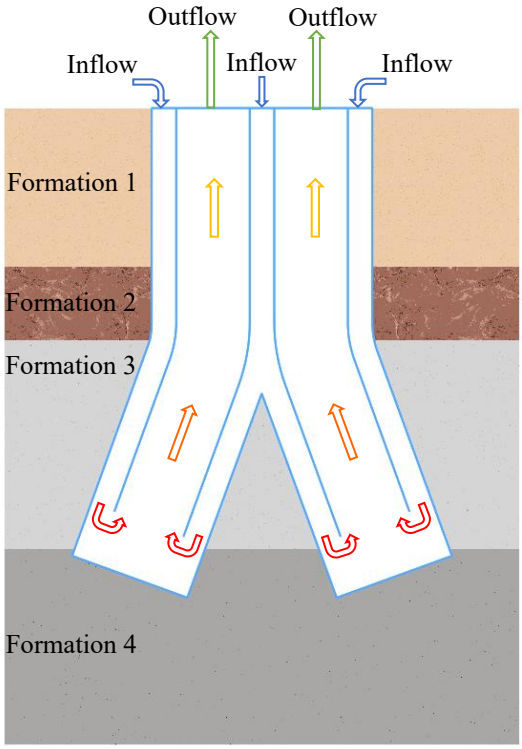

Fig.2 Simplified closed-loop heat extraction model for symmetrically arranged two deviated-geothermal wells

Table 1 Main parameters of the three closed-loop models used in the simulation

Name	Pipe name	Size (mm)	Depth (m)
Model A & Model B	Inner pipe	Ø100	1998
	Outer pipe	Ø159.42	2000
Model C	Inner pipe	2 × Ø70.71	1998
	Outer pipe	Ø159.42	2000

Table 2 Formation properties [9]

Formation Layer	Depth (m)	Density ($kg \cdot m^{-3}$)	Specific heat capacity ($J \cdot kg^{-1} \cdot K^{-1}$)	Thermal conductivity ($W \cdot m^{-1} \cdot K^{-1}$)
Formation 1	0-500	1760	1433	1.59
Formation 2	500-720	1860	1025	1.65
Formation 3	720-1450	2070	878	1.76
Formation 4	1450-2000	2270	848	1.88

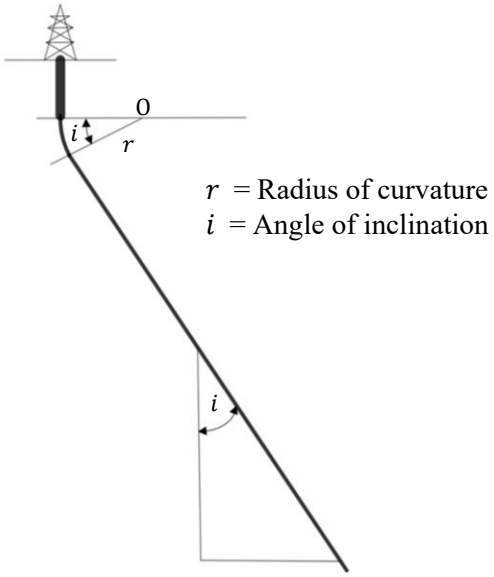

Fig.3 Deviated geothermal well tracks [10]

Table 3 Comparison between measured and simulated results

Region	Cai [9]
Well depth (m)	2000
Mass flow (kg/s)	7.77
Inlet temperature (°C)	17.3
Measured outflow temperature (°C)	26.1
Simulated outflow temperature (°C)	24.8

Table 3. It can be seen from Table 3 that the simulated outflow temperatures are quite close to the measured data, the deviation percentage is 4.98%, which is acceptable. Since no experimental data of deviated wells have been found, validation for the Model B and Model C could not be done but with assumption that the Model B and Model C also work.

3. SIMULATION RESULTS

3.1 Outlet temperature variations

To investigate the heat extraction performance of the three closed-loop models (Model A, B, and C), the simulated heating season was chosen as 120 days. The ground temperature and the inflow temperature were set to be 20°C. The mass flow rates investigated were 1kg/s, 2kg/s, 3kg/s, and 4kg/s respectively. The geothermal gradient was set by using user defined functions in Fluent. All three models were run under realizable k- ε model. The turbulence specification

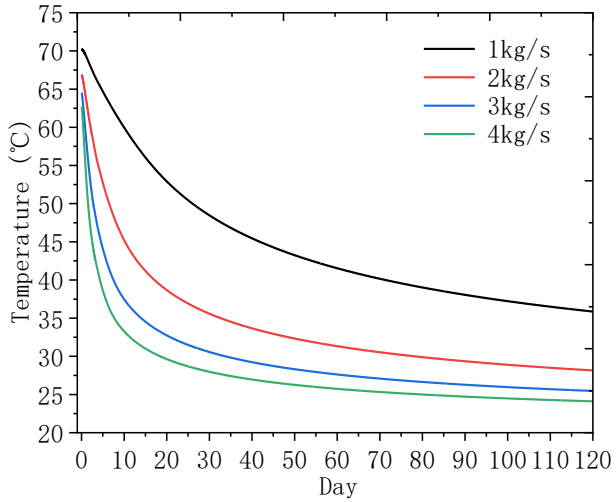

(a) Model A

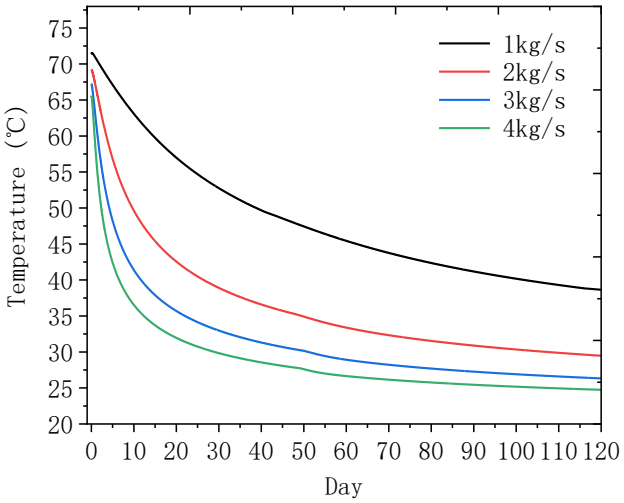

(b) Model B

Fig.4 Outlet temperature changes with heat extraction time under different mass flow rate conditions (a) Model A (b) Model B

method of inlets was chosen to be intensity and hydraulic diameter, and the solution method scheme was chosen to be SIMPLEC. The heat extraction performances have been compared among the three closed-loop models in terms of their mass flowrates' influence.

Fig.4 shows the changes of outlet temperature of Model A and Model B under different mass flowrates. It can be seen that after 120 days, the outlet temperatures of Model A become 35.9°C, 28.2°C, 25.5°C and 24.1°C, respectively, and the outlet temperatures of Model B become 38.8°C, 29.5°C, 26.3°C and 24.8°C respectively, corresponding to the mass flowrates of 1 kg/s, 2 kg/s, 3 kg/s and 4 kg/s in each case. The outlet temperature of the two models dropped obviously when the mass flowrate increased from 1 kg/s to 2 kg/s, but the temperature drop was not so obvious from 2 kg/s to 4 kg/s. It is noticed that the outlet temperature of Model B is higher than that of Model A under each mass flowrate condition, but this becomes less obvious if the mass flowrate becomes higher; the outlet temperature of Model B is only 0.8°C or 0.7°C (3.04% and 2.9%) higher than that of the Model A, corresponding to a mass flowrate of 3 kg/s or 4 kg/s respectively.

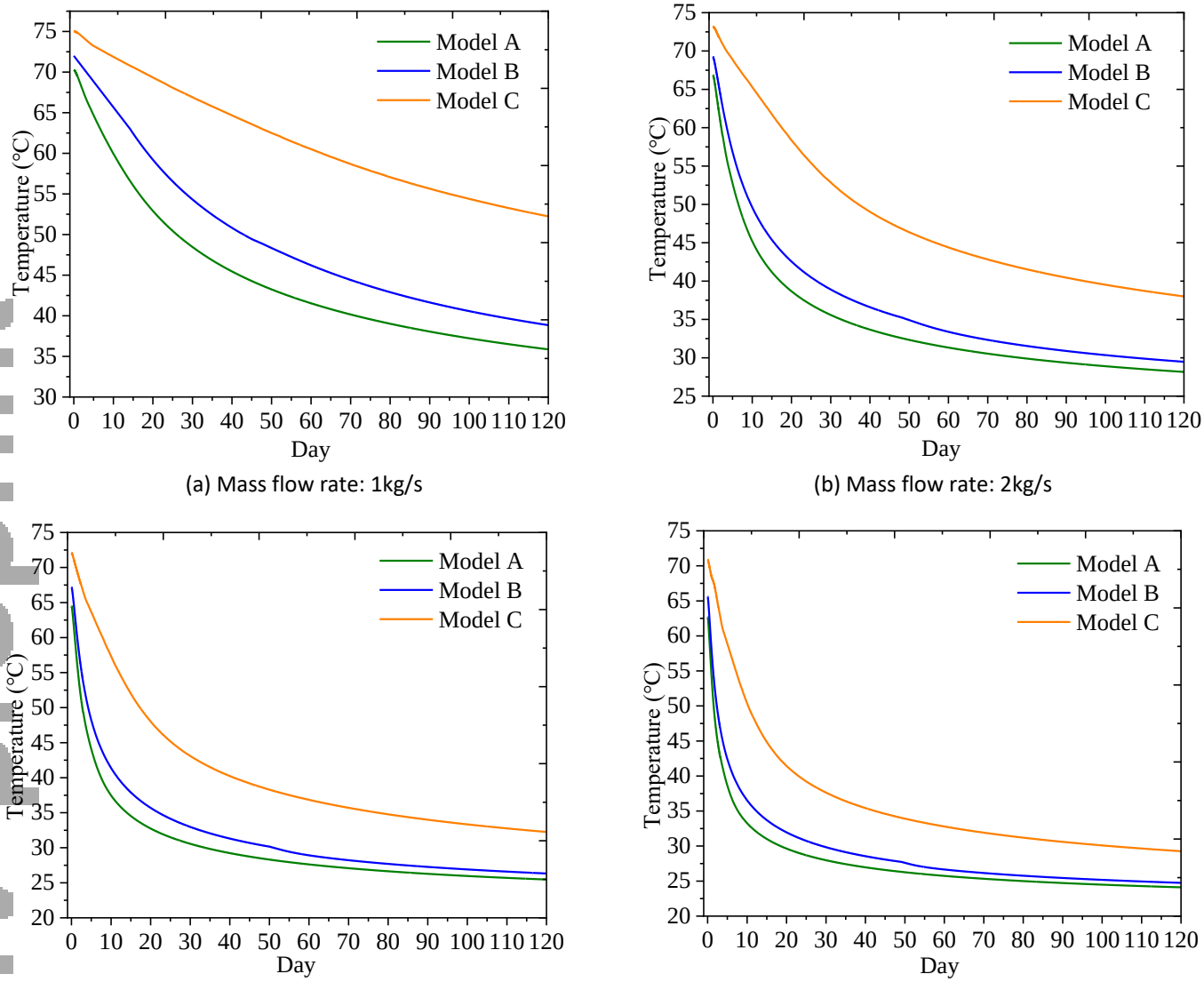

(a) Mass flow rate: 1kg/s

(b) Mass flow rate: 2kg/s

(c) Mass flow rate: 3kg/s

(d) Mass flow rate: 4kg/s

Fig.5 Outlet temperature changes of the three closed-loop models under different mass flow rate conditions

Fig.5 shows the changes of the outlet temperature of the three models under different mass flowrate conditions. As can be seen, the outlet temperatures of Model C are 52.2°C, 38.0°C, 32.3°C and 29.3°C respectively corresponding to mass flowrate of 1kg/s, 2kg/s, 3kg/s, and 4kg/s at the end of 120 days. The outlet

temperature of Model C is 8.1°C (27.1%) higher than that of the Model B and 9.5°C (33.5%) higher than that of Model A on average. Because the heat transfer area of Model C has greatly increased, more heat can be extracted in this case. It is worth noting that the outlet temperature of Model C drops very slowly when the mass flowrate is 1 kg/s. However, it drops much quicker when the mass flowrate is greater than 2kg/s. This is not difficult to understand because a greater mass flowrate means a greater velocity which leads to a higher heat transfer coefficient and results in a higher heat extraction rate. The greater the heat transfer rate in the well, the quicker the temperature drop in the formation, causing a decrease of the outlet temperature.

3.2 Heat extraction rates and optimum mass flowrates

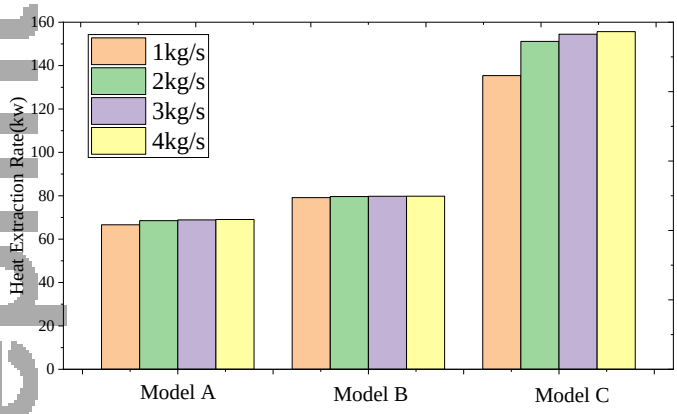

Fig.6 Heat extraction rates of the wells at the end of four months under different mass flowrate conditions

Fig.6 shows the heat extraction rates (geothermal energy production rates) of the three closed-loop models under different mass flowrate conditions. At the end of 120 days, the heat extraction rates of Model A are 66.63 kW, 68.51 kW, 68.88 kW and 69.05 kW corresponding to the mass flowrates of 1 kg/s, 2 kg/s, 3 kg/s and 4 kg/s respectively. Since increasing the mass flowrate from 2kg/s to 3kg/s or 4kg/s has almost no contribution to its heat extraction rate, the optimum mass flowrate in this scenario is considered to be 2kg/s. In the scenario of Model B, the corresponding heat extraction rates are 79.14 kW, 79.63 kW, 79.76 kW and 79.8 kW, a 18.78%, 16.23%, 15.80% and 15.59% increase compared with that of Model A. As the heat extraction rate has almost no change with the increase of the mass flowrate, the optimum mass flowrate in this scenario is 1kg/s. In the scenario of Model C, the heat extraction rates are 135.4 kW, 151.17 kW, 154.48 kW and 155.65 kW respectively, corresponding to a 103.21%, 120.65%, 124.27% and 125.42% increase compared with Model A and a 71.09%, 89.84%, 93.68% and 95.05% increase compared with Model B. From Fig.6 and the calculation results, it can be seen that the heat extraction rates increase slightly from Model A to Model B, but they increase remarkably from Model B to Model C. Since the mass flowrate greater than 3kg/s has little contribution to the increase of heat extraction rates of Model C, its optimum mass flowrate is considered to be around 3 kg/s.

4. CONCLUSIONS

In this study, performances of closed-loop heat extraction from a deviated geothermal well (Model B) and symmetrically arranged two deviated-geothermal wells (Model C) have been investigated and compared with the that from a vertical geothermal well (Model A). The main conclusions are as follows:

(1) With the increase of the mass flowrate from 1 kg/s to 4 kg/s, the outlet temperatures of the three models all decrease after four months operation. Model C has the highest outlet temperature, which is approximately 8.1°C (27.1%) higher than that of Model B and 9.5°C (33.5%) higher than that of Model A on average.

(2) The heat extraction rate of Model B is slightly higher than that of Model A under the same mass flowrate. Whereas, the heat extraction rate of Model C is much higher than that of Model A or B; when the mass flowrate is 3 kg/s, the corresponding growth rate is about 124% and 94% respectively.

(3) Based on the analysis of each Model's heat extraction rate, the optimum mass flowrates of Model A, Model B and Model C in this study are 2 kg/s, 1 kg/s and 3 kg/s respectively.

5. DISCUSSION

Further studies will focus on the quadruple-deviated geothermal wells to verify its better performance than the double-deviated one. And the studies on techno-economic analysis will be carried out in determining the optimum well spacing, well patterns, the mass flowrate and the corresponding heat extraction rate in a certain geothermal field with considerations of the drilling cost, heating benefits and electricity prices, etc.

ACKNOWLEDGEMENT

This work was supported by the National Key Research and Development Program of the 13th Five-Year Plan of China (grant number 2018YFB1501805).

REFERENCE

[1] K. Wang , B. Yuan , G. Ji , et al. A comprehensive review of geothermal energy extraction and utilization in oilfields. Journal of Petroleum ence and Engineering, 2018, 168:465-477.

[2] Shortall R, Davidsdottir B, Guðni Axelsson, et al. Geothermal energy for sustainable development: A review of sustainability impacts and assessment frameworks. Renewable & Sustainable Energy Reviews, 2015, 44(C):391-406.

[3] J. Zhu , K. Hu , X. Lu , et al. A review of geothermal energy resources, development, and applications in China: Current status and prospects. Energy, 2015, 93:466-483.

[4] P. Jiang , X.Li , R. Xu , et al. Heat extraction of novel underground well pattern systems for geothermal energy exploitation. Renewable Energy, 2016, 90:83-94.

[5] Rybach L , Hopkirk R J. 1995. Shallow and deep borehole heat exchangers - achievements and prospects. // Proc. World Geothermal Congress. International Geothermal Association. Florence, Italy, 2133-2138

[6] Alimonti C , Soldo E . Study of geothermal power generation from a very deep oil well with a wellbore heat exchanger. Renewable Energy, 2016, 86:292-301.

[7] X. Bu , W. Ma , H. Li . Geothermal energy production utilizing abandoned oil and gas wells. Renewable Energy, 2012, 41:80-85.

[8] Noorollahi Y , Pourarshad M , Jalilinasrabady S , et al. Numerical simulation of power production from abandoned oil wells in Ahwaz oil field in southern Iran. Geothermics, 2015, 55:16-23.

[9] W. Cai , F. Wang , J. Liu , et al. Experimental and numerical investigation of heat transfer performance and sustainability of deep borehole heat exchangers coupled with ground source heat pump systems. Applied Thermal Engineering, 2018.

[10] Sadiq J. Zarrouk, Katie McLean, Chapter 3: Geothermal wells. In: Geothermal Well Test Analysis, London, Academic Press, 2019, p. 39-61.